

On the Importance of Electroweak Corrections for Majorana Dark Matter Indirect Detection

Paolo Ciafaloni ^a, Marco Cirelli ^{b,c}, Denis Comelli ^d
Andrea De Simone ^e, Antonio Riotto ^{b,f}, Alfredo Urbano ^{a,g}

^a *Dipartimento di Fisica, Università di Lecce and INFN - Sezione di Lecce,
Via per Arnesano, I-73100 Lecce, Italy*

^b *CERN, PH-TH Division, CH-1211, Genève 23, Switzerland*

^c *Institut de Physique Théorique, CNRS URA 2306
and CEA/Saclay, F-91191 Gif-sur-Yvette, France*

^d *INFN - Sezione di Ferrara, Via Saragat 3, I-44100 Ferrara, Italy*

^e *Institut de Théorie des Phénomènes Physiques,
École Polytechnique Fédérale de Lausanne, CH-1015 Lausanne, Switzerland*

^f *INFN, Sezione di Padova, Via Marzolo 8, I-35131, Padova, Italy*

^g *IFAE, Universitat Autònoma de Barcelona, 08193 Bellaterra, Barcelona, Spain*

Abstract

Recent analyses have shown that the inclusion of electroweak corrections can alter significantly the energy spectra of Standard Model particles originated from dark matter annihilations. We investigate the important situation where the radiation of electroweak gauge bosons has a substantial influence: a Majorana dark matter particle annihilating into two light fermions. This process is in p -wave and hence suppressed by the small value of the relative velocity of the annihilating particles. The inclusion of electroweak radiation eludes this suppression and opens up a potentially sizeable s -wave contribution to the annihilation cross section. We study this effect in detail and explore its impact on the fluxes of stable particles resulting from the dark matter annihilations, which are relevant for dark matter indirect searches. We also discuss the effective field theory approach, pointing out that the opening of the s -wave is missed at the level of dimension-six operators and only encoded by higher orders.

1 Introduction

In a recent paper [1] some of us have pointed out that the energy spectra of the Standard Model (SM) particles originating from Dark Matter (DM) annihilation/decays can be significantly affected by ElectroWeak (EW) corrections, if the mass M of the DM particles is larger than the EW scale (here set to be the mass of the W boson m_W). The emission of EW gauge bosons from the final state of the annihilation/decay process is enhanced by single logarithms $\ln M^2/m_W^2$ in the collinear region and by double logarithms $\ln^2 M^2/m_W^2$ when both collinear and infrared singularities are present, and implies that all stable particles of the SM appear in the final spectrum, independently of the primary annihilation/decay channel. The inclusion of EW corrections seems therefore an essential ingredient in indirect searches for DM. The impact of EW corrections is particularly relevant in two situations: (1) when one is interested in the energy region of the final fluxes (after propagation from the source) which corresponds to the low-energy tail of the spectrum, populated by the decay products of the additional gauge bosons; (2) when some of the stable species appear only if EW corrections are taken into account, for instance antiprotons (from W or Z decays) in an otherwise purely leptonic annihilation.

One basic assumption made in Ref. [1] was that the tree-level $2 \rightarrow 2$ annihilation cross section of the DM particles into SM states was dominant over the $2 \rightarrow 3$ cross section with soft gauge boson emission from the external legs, and the latter was factorized with respect to the former.

While this assumption is certainly reasonable and commonly made (for instance if the DM is a heavy Dirac fermion singlet under the SM gauge group), there are well-motivated cases in which it is questionable. Consider for instance a DM particle χ which is a Majorana fermion and a SM singlet. The cross section of $\chi\chi \rightarrow f\bar{f}$, where DM annihilates into SM fermions of mass m_f , consists of a velocity-independent (s -wave) and a velocity-dependent (p -wave) contribution

$$v\sigma = a + bv^2 + \mathcal{O}(v^4), \quad (1.1)$$

where $v \sim 10^{-3}$ is the relative velocity (in units of c) of the DM states in our Galaxy. By helicity arguments, $a \propto (m_f/M)^2$ and hence very suppressed for light final state fermions (e.g. leptons), while the p -wave term is suppressed by v^2 . In this case, it is not guaranteed that the 2-body annihilation cross section is quantitatively larger than the one with EW corrections. Indeed, the latter ones may open a sizeable s -wave contribution and elude the suppressions.

The scope of this paper is therefore to generalize the results of Ref. [1] to the interesting case in which the 2-body annihilation cross-section is not automatically larger than the one with soft gauge boson emission. The same kind of effect has been considered in the past with respect to photon radiation in Refs. [2–4]; this work is partly, but not only, an extension of those analyses to include also W, Z gauge bosons. On the other hand, an approach similar to ours is the one carried out in Ref. [5], but our final results disagree with the ones published

there ¹. Other works which considered at various levels the impact of EW corrections on DM annihilation or cosmic ray physics include [6]. For somewhat related work on 3-body annihilations below threshold see also Ref. [7].

We shall show in detail that, whenever the dark matter annihilation occurs by exchange of a heavy intermediate state, at the lowest order in the expansion in inverse powers of this heavy mass, final state radiation is not sufficient to remove the helicity suppression, while it is efficiently removed at higher orders by processes involving the emission both from external legs and from virtual internal propagators. Although subleading in terms of powers of the heavy mass, these contributions do not pay the velocity suppression and actually can be dominant.

This allows us to raise an important and cautionary remark concerning the use of the effective field theory approach to describe DM interactions [8]. If the interactions of DM with SM fermions are described by effective four-fermion dimension-six operators, then the emission of soft gauge bosons can only take place at the lowest order from the external legs and the corresponding cross section remains helicity suppressed. In other words, the effect of opening up a large *s*-wave annihilation channel is missed at the level of dimension-six operators and then one may (incorrectly) conclude that the whole cross section is still suppressed. Instead, as we shall point out, the diagrams leading to *s*-wave contributions correspond to operators with dimension higher than six, whose quantitative relevance for the cross section can be comparable or larger than that due to dimension-six operators, despite the larger dimensionality.

The plan of the paper is as follows. In Section 2 we describe the simple model we shall use throughout the paper. Then, Section 3 introduces preliminary considerations about 2-body annihilations, especially about helicity-suppression, setting the ground for the subsequent discussion. Section 4 contains the calculations and the results for the annihilation cross section with the inclusion of EW bremsstrahlung (including the Ward Identities check and the remarks on the effective field theory approach). Our results for the 3-body cross sections are in disagreement with those of Ref. [5], while we find a perfect agreement with those in Ref. [2] concerning the radiation of one photon. With these analytical results at hand, we are then ready to study in detail the impact of the opening of the *s*-wave on the fluxes of stable SM particles. To this end, we carry out a numerical analysis. In Section 5, we derive the energy spectra at production while in Section 6 these spectra are then propagated to give the fluxes of particles at detection. Concluding remarks are collected in Section 7.

2 The model

In this section we present the (toy) model we shall use in the paper to describe the relevance of the EW corrections in DM annihilations. Let us add to the particle content of the SM a Majorana spinor χ with mass M_χ , singlet under the SM gauge group and playing the role of

¹The disagreement originates from the use of incorrect Fierz identities, thus invalidating the calculation of the cross sections, as we have been informed by the authors of Ref. [5] in a private communication.

DM, and a scalar $SU(2)$ -doublet S , with mass $M_S > M_\chi$

$$\chi = \chi^C \quad S = \begin{pmatrix} \eta^+ \\ \eta^0 \end{pmatrix}. \quad (2.1)$$

The field S provides the interactions of the DM with the generic fermion of the SM, described by the left-handed doublet $L = (f_1, f_2)$. In fact, the total Lagrangian of the model is (see also Ref. [9])

$$\mathcal{L} = \mathcal{L}_{\text{SM}} + \mathcal{L}_\chi + \mathcal{L}_S + \mathcal{L}_{\text{int}}, \quad (2.2)$$

where to the Standard Model Lagrangian \mathcal{L}_{SM} we added

$$\mathcal{L}_\chi = \frac{1}{2} \bar{\chi} (i\partial - M_\chi) \chi, \quad (2.3)$$

$$\mathcal{L}_S = (D_\mu S)^\dagger (D^\mu S) - M_S^2 S^\dagger S, \quad (2.4)$$

$$\mathcal{L}_{\text{int}} = y_L \bar{\chi} (L i\sigma_2 S) + \text{h.c.} = y_L (\bar{\chi} P_L f_2 \eta^+ - \bar{\chi} P_L f_1 \eta^0) + \text{h.c.}, \quad (2.5)$$

where the 4-component notation has been used and where contractions on $SU(2)$ indices is defined as $(L i\sigma_2 S) \equiv L_i (i\sigma_2)_{ij} S_j$. Moreover, we shall adopt the convention for projectors: $P_{R,L} = (1 \pm \gamma^5)/2$. The stability of the DM can be achieved e.g. by endowing χ and S with odd parity under a Z_2 symmetry, while the rest of the SM spectrum is even.

The model is manifestly gauge invariant, and is the same of Ref. [5], which will allow us a direct comparison between their results and ours. A reader expert in supersymmetry would recognize the same interactions of a Bino with fermions and their supersymmetric scalar partners.

We shall restrict our attention to the massless limit $m_{f_1} = m_{f_2} = 0$. While reasonable for leptons and light quarks, this approximation may not be good for heavy quarks. For instance, the DM annihilation into $t\bar{t}$, if kinematically allowed, would proceed through s -wave with a contribution proportional to $(m_t/M_\chi)^2$, which can be large already without EW corrections. However, the generalization of our calculations to non-zero fermion masses is beyond the scope of this paper.

As anticipated in the Introduction, one of the main goals of the present paper is to show that the inclusion of higher-order processes with emission of soft weak gauge bosons evades the helicity suppression and turns on an unsuppressed s -wave contribution to the DM annihilation cross section. Before turning to the details of the calculation of the $2 \rightarrow 3$ scatterings in Section 4, let us first review some standard material about $2 \rightarrow 2$ annihilations, with particular emphasis on the role of helicity suppression. This will serve to set the notation and to highlight the main points for later use. The analogous results for the amplitudes and the cross sections of the 2-body and 3-body processes in the case of Dirac DM are reported in Appendix A.

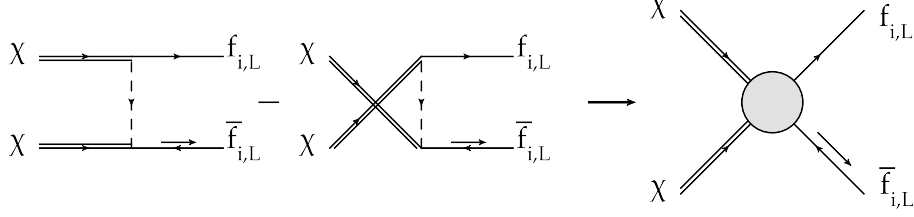


Figure 1: *Feynman diagrams for the tree-level annihilation in Eq. (3.1) together with its effective contraction in the limit $M_S \gg M_\chi$.*

3 Two-body annihilation into fermions and the helicity suppression

Let us consider the annihilation of the DM Majorana fermion into a pair of massless left-handed fermions (see Figure 1)

$$\chi(k_1)\chi(k_2) \rightarrow f_{L_i}(p_1)\bar{f}_{L_i}(p_2). \quad (3.1)$$

The cross section admits the usual expansion in powers of the relative velocity v of the initial DM particles

$$v\sigma = a + bv^2 + \mathcal{O}(v^4), \quad (3.2)$$

where the coefficients a, b corresponding to s - and p -waves, respectively, are given by

$$a = 0, \quad b = \frac{|y_L|^4}{48\pi} \frac{1+r^2}{(1+r)^4} \frac{1}{M_\chi^2}, \quad (3.3)$$

where we have defined

$$r \equiv \frac{M_S^2}{M_\chi^2}. \quad (3.4)$$

This result shows the well-known fact that the first non-zero contribution to the tree-level cross section for the Majorana DM is velocity dependent, and hence suppressed.

Let us try to understand this fact in simple terms. At the level of Feynman diagrams the Majorana nature of the DM implies the presence of two crossed channels, t and u (for Dirac DM, only the t -channel contribution would be present). The amplitudes are of the form $(\bar{\chi}P_L f)(\bar{f}P_R\chi)$, which becomes $(\bar{\chi}\gamma_\alpha P_R\chi)(\bar{f}\gamma^\alpha P_L f)$ after chiral Fierz transformation. The total tree-level amplitude for the process in Eq. (3.1) is given by

$$\mathcal{M}_0 = \frac{i|y_L|^2}{2} [\bar{u}_f(p_1) \gamma_\alpha P_L v_f(p_2)] \left[\frac{D_{11} - D_{12}}{2} \bar{v}_\chi(k_2) \gamma^\alpha u_\chi(k_1) + \frac{D_{11} + D_{12}}{2} \bar{v}_\chi(k_2) \gamma^\alpha \gamma_5 u_\chi(k_1) \right], \quad (3.5)$$

where we have defined the quantities

$$D_{ij} \equiv \frac{1}{(p_i - k_j)^2 - rM_\chi^2}, \quad (3.6)$$

which satisfy the property $D_{i1} - D_{i2} = 2 p_i \cdot (k_1 - k_2) D_{i1} D_{i2}$. Notice that the momenta of the incoming DM particles are such that $k_1^\mu - k_2^\mu \sim \mathcal{O}(v) M_\chi$. We thus obtain that

$$D_{i1} - D_{i2} \sim \mathcal{O}(v) M_\chi^2 D_{i1} D_{i2}. \quad (3.7)$$

In the matrix element in Eq. (3.5), the first term represents a vector current while the second term is an axial-vector current. Let us analyze the velocity factors present in each of them, in the non-relativistic limit $v \ll 1$. The vector current is multiplied by a factor proportional to v due to Eq. (3.7). For the axial current of Eq. (3.5), using the Gordon identities we have

$$\bar{v}_\chi(k_2) \gamma^\alpha \gamma_5 u_\chi(k_1) = -\frac{k_1^\alpha + k_2^\alpha}{2M_\chi} \bar{v}_\chi(k_2) \gamma_5 u_\chi(k_1) - \frac{i}{2M_\chi} \bar{v}_\chi(k_2) \sigma^{\alpha\beta} (k_{1\beta} - k_{2\beta}) \gamma_5 u_\chi(k_1) \quad (3.8)$$

The vector $(k_1 + k_2)^\alpha = (p_1 + p_2)^\alpha$ in the first term saturates the current $\bar{u}_f \gamma_\alpha P_L v_f$ in Eq. (3.5) and gives rise to terms proportional to the fermion mass, which are zero in our computation. The second term gives again an $\mathcal{O}(v)$ contribution. We thus recovered the well-known fact that for Majorana fermions the scattering amplitude is proportional to the first power of the relative velocity of the incoming particles. Notice that for Dirac DM Eq. (3.5) would not contain the D_{21} terms, as only the t -channel contributes to the amplitude, and the vector current thus gives rise to an unsuppressed s -wave term in the cross section (see App. A for details).

Another interesting limit to analyze is the large scalar mass regime $r \gg 1$ for which

$$D_{ij} \sim \frac{1}{r M_\chi^2} \left[1 + \mathcal{O}\left(\frac{1}{r^2}\right) \right] \quad \text{and} \quad D_{i1} - D_{i2} \sim \mathcal{O}\left(\frac{v}{r^2}\right) \frac{1}{M_\chi^2}. \quad (3.9)$$

In this case, the amplitude for DM Majorana annihilation into (massless) fermions at leading order in v and $1/r$ is given by Eq. (3.5), where the first term in square brackets is $\mathcal{O}(v/r^2)/M_\chi^2$, which is subdominant with respect to the second one, of order $[\mathcal{O}(v/r)/M_\chi^2][\bar{v}_\chi \sigma^{\alpha 3} \gamma_5 u_\chi]$; thus, the tree-level cross section will approximately be given by

$$v\sigma(\chi\chi \rightarrow f\bar{f}) \sim \frac{1}{M_\chi^2} \frac{v^2}{r^2}. \quad (3.10)$$

4 Three-body DM Annihilation

Let us now turn to analyze the case of interest, namely the emission of EW gauge bosons in DM annihilations. First, we are going to manipulate the matrix element and discuss its velocity dependence. Then, we deal with the kinematical constraints of the 3-body phase space and arrive at the results for the cross section. Finally, we re-interpret our findings in the language of effective field theory and make some remarks about its use.

4.1 Matrix element and velocity dependence

Let us discuss for definiteness the 3-body process with the emission of a Z boson

$$\chi(k_1) \chi(k_2) \rightarrow \bar{f}_L(p_2) f_L(p_1) Z(k). \quad (4.1)$$

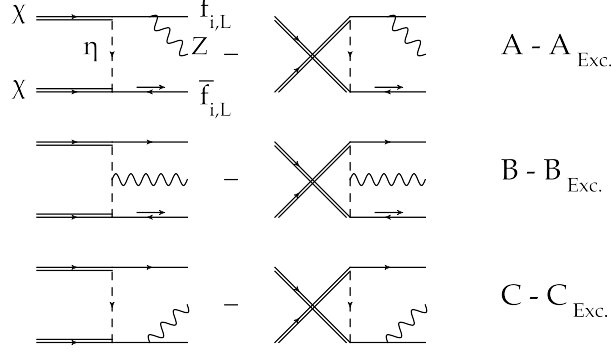


Figure 2: *Feynman diagrams for the 3-body process in Eq. (4.1).*

The corresponding Feynman diagrams are depicted in Figure 2. Of course, we shall include also the emission of W gauge bosons in the final results. The amplitude can be written as

$$i\mathcal{M} \cdot \epsilon^* = \frac{ig|y_L|^2(1-2s_W^2)}{4c_W} [(\mathcal{M}_A - \mathcal{M}_A^{\text{exc}}) + (\mathcal{M}_B - \mathcal{M}_B^{\text{exc}}) + (\mathcal{M}_C - \mathcal{M}_C^{\text{exc}})], \quad (4.2)$$

where we have denoted $s_W \equiv \sin \theta_W$ and $c_W \equiv \cos \theta_W$, being θ_W the Weinberg angle. Following e.g. Ref. [3], we shall call “FSR” (final state radiation) the processes where a gauge boson is radiated from an external leg, while we refer to the emission from internal virtual particles as “VIB” (virtual internal bremsstrahlung). Thus, the A and C terms are of FSR type, while the B terms are VIB.

In order to show how the Fierz transformation works, let us analyze in more detail the amplitude \mathcal{M}_A , for massless outgoing fermions

$$\mathcal{M}_A = \frac{2[\bar{u}_f(p_1)\not{\epsilon}^*(k)P_L(\not{p}_1 + \not{k})u_\chi(k_1)][\bar{v}_\chi(k_2)P_L v_f(p_2)]}{(2p_1 \cdot k + m_Z^2)(M_\chi^2(1-r) - 2p_2 \cdot k_2)}, \quad (4.3)$$

where each fermionic current is composed by a Dirac and a Majorana spinor, for f and χ respectively. Applying the Fierz transformation

$$(P_R)_{ij}(P_L)_{kl} = \frac{1}{2}(P_R\gamma^\mu)_{il}(P_L\gamma_\mu)_{kj}, \quad (4.4)$$

we can perform the rearrangement

$$\begin{aligned} & \bar{v}_\chi(k_2)_i(P_L)_{ij}v_f(p_2)_j[\bar{u}_f(p_1)\gamma^\rho(\not{p}_1 + \not{k})_k(P_R)_{kl}u_\chi(k_1)_l] \\ &= \frac{1}{2}[\bar{v}_\chi(k_2)P_L\gamma^\mu u_\chi(k_1)][\bar{u}_f(p_1)\gamma^\rho(\not{p}_1 + \not{k})P_R\gamma_\mu v_f(p_2)]. \end{aligned} \quad (4.5)$$

so that Eq. (4.3) becomes

$$\mathcal{M}_A = \frac{[\bar{u}_f(p_1)\not{\epsilon}^*(k)(\not{p}_1 + \not{k})P_R\gamma_\mu v_f(p_2)][\bar{v}_\chi(k_2)P_L\gamma^\mu u_\chi(k_1)]}{(2p_1 \cdot k + m_Z^2)(M_\chi^2(1-r) - 2p_2 \cdot k_2)}. \quad (4.6)$$

With the same technique, the terms in the total amplitude (4.2) read

$$\mathcal{M}_A - \mathcal{M}_A^{\text{exc}} = \frac{\bar{u}_f \not{\epsilon}^*(k) (\not{p}_1 + \not{k}) P_R \gamma^\mu v_f}{2p_1 \cdot k + m_Z^2} \cdot \left(\frac{D_{22} - D_{21}}{2} \bar{v}_\chi \gamma_\mu u_\chi + \frac{D_{22} + D_{21}}{2} \bar{v}_\chi \gamma_\mu \gamma_5 u_\chi \right), \quad (4.7)$$

$$\begin{aligned} \mathcal{M}_B - \mathcal{M}_B^{\text{exc}} &= (-1) [\bar{u}_f P_R \gamma^\mu v_f] [(k_1 - k_2 - p_1 + p_2) \cdot \epsilon^*(k) \bar{v}_\chi P_L \gamma_\mu u_\chi D_{11} D_{22} \\ &\quad - (k_2 - k_1 - p_1 + p_2) \cdot \epsilon^*(k) \bar{v}_\chi \gamma_\mu P_L u_\chi D_{21} D_{12}], \end{aligned} \quad (4.8)$$

$$\mathcal{M}_C - \mathcal{M}_C^{\text{exc}} = -\frac{\bar{u}_f P_R \gamma^\mu (\not{p}_2 + \not{k}) \not{\epsilon}^*(k) v_f}{2p_2 \cdot k + m_Z^2} \cdot \left(\frac{D_{11} - D_{12}}{2} \bar{v}_\chi \gamma_\mu u_\chi + \frac{D_{11} + D_{12}}{2} \bar{v}_\chi \gamma_\mu \gamma_5 u_\chi \right). \quad (4.9)$$

Let us now discuss the limit $v \ll 1$ and $r \gg 1$, in analogy with the previous section for the 2-body process. The coefficient of the DM *vector* current in the full amplitudes of the kind A , B and C is always $\mathcal{O}(v)$ as it happens for the 2-body case, due to Eq. (3.7); in particular, in the large r limit it is proportional to $\mathcal{O}(v/r^2)/M_\chi^2$ (as in Eq. (3.9)). Instead, for the *axial-vector* current, the crucial point is that the mass cancellation of order $\mathcal{O}(m_f)$ does not occur anymore. Indeed, from the Gordon identities we recover Eq. (3.8), where the second term turns out to be proportional to v , while in the first term the 4-vector saturating the fermionic currents is now $(p_1 + p_2 + k)_\mu$, which does not trigger anymore the chiral identity, and leaves non-zero terms even for vanishing m_f . Thus, the terms of the amplitudes containing $\bar{v}_\chi \gamma_5 u_\chi$ read

$$(\mathcal{M}_A - \mathcal{M}_A^{\text{exc}} + \mathcal{M}_C - \mathcal{M}_C^{\text{exc}})|_{\bar{v}_\chi \gamma_5 u_\chi} = [\bar{u}_f \not{\epsilon}^* P_L v_f] \frac{[\bar{v}_\chi \gamma_5 u_\chi]}{2M_\chi} \underbrace{\frac{(D_{22} + D_{21}) - (D_{11} + D_{12})}{2}}_{\mathcal{O}(\frac{1}{r^2}) \frac{1}{M_\chi^2}} \quad (4.10)$$

$$\begin{aligned} (\mathcal{M}_B - \mathcal{M}_B^{\text{exc}})|_{\bar{v}_\chi \gamma_5 u_\chi} &= -[\bar{u}_f \not{k} P_L v_f] \frac{[\bar{v}_\chi \gamma_5 u_\chi]}{2M_\chi} \left[(p_2 - p_1) \cdot \epsilon^*(k) \underbrace{\frac{(D_{11} D_{22} + D_{12} D_{21})}{2}}_{\mathcal{O}(\frac{1}{r^2}) \frac{1}{M_\chi^4}} + \right. \\ &\quad \left. \underbrace{\frac{(k_1 - k_2) \cdot \epsilon^*(k)}{v M_\chi \epsilon_z^*}}_{\mathcal{O}(\frac{v}{r^3}) \frac{1}{M_\chi^4}} \underbrace{\frac{(D_{11} D_{22} - D_{12} D_{21})}{2}}_{\mathcal{O}(\frac{v}{r^3}) \frac{1}{M_\chi^4}} \right], \end{aligned} \quad (4.11)$$

where we have highlighted the behavior of each term with v and $1/r$. Notice that now there appear terms without v dependence. Indeed, in the limit $v = 0$ and to leading order in $1/r \ll 1$, the full amplitude is given by

$$\mathcal{M}|_{v \rightarrow 0} = \frac{(\bar{v}_\chi \gamma_5 u_\chi)}{2M_\chi^5} \frac{1}{r^2} [(\bar{u}_f \not{\epsilon}^* P_L v_f) (p_1 - p_2) \cdot (k_1 + k_2) - (\bar{u}_f \not{k} P_L v_f) (p_2 - p_1) \cdot \epsilon^*], \quad (4.12)$$

where the first term comes from FSR while the second originates from VIB, and they are both of order $\mathcal{O}(1/r^2)$. Schematically, the various contributions to the amplitude can be organized

as follows

$$\mathcal{M} \sim \frac{1}{M_\chi} \mathcal{O}(v) \left[\mathcal{O}\left(\frac{1}{r}\right)\Big|_{\text{FSR}} + \mathcal{O}\left(\frac{1}{r^2}\right)\Big|_{\text{FSR}} \right] + \frac{1}{M_\chi} \left[\mathcal{O}\left(\frac{1}{r^2}\right)\Big|_{\text{VIB}} + \mathcal{O}\left(\frac{1}{r^2}\right)\Big|_{\text{FSR}} \right]. \quad (4.13)$$

At this point we can learn an important lesson (see also Ref. [2]): the opening of the s -wave originates from diagrams of both FSR and VIB type, at $\mathcal{O}(1/r^2)$ in the amplitude; limiting the expansion up to $\mathcal{O}(1/r)$ in the amplitude would cause the process to stay in the p -wave.

An order-of-magnitude estimate for the 3-body cross section, showing the leading dependence on the expansion parameters, can be obtained straightforwardly

$$v\sigma(\chi\chi \rightarrow f\bar{f}Z) \sim \frac{\alpha_W}{M_\chi^2} \left[\mathcal{O}\left(\frac{v^2}{r^2}\right) + \mathcal{O}\left(\frac{v^2}{r^3}\right) + \mathcal{O}\left(\frac{1}{r^4}\right) \right], \quad (4.14)$$

where the weak coupling $\alpha_W = g^2/(4\pi)$ for the gauge boson emission has been restored. The estimates in Eqs. (3.10) and (4.14) allow to gather an understanding in simple terms of the situation we are studying. While the 2-body annihilation cross section behaves like v^2/r^2 , the 3-body FSR and VIB diagrams give rise to both s -wave and p -wave terms. The p -wave from 3-body processes cannot compete with the 2-body cross section because of the extra α_W factor; however the s -wave from $2 \rightarrow 3$ annihilation, free from the v^2 suppression, can overcome the $2 \rightarrow 2$ cross section if r is not too large. In the next subsection we shall give a more precise estimate based on the analytical results.

Because of the importance of this point, and being the distinction between FSR and VIB not able to disentangle clearly the s -wave contribution from the p -wave one, let us introduce now a specific notation. Having in mind an expansion in powers of $1/r$ in the amplitude – as sketched in Eq. (4.13) – we shall call “leading order” (LO) the lowest order term $\mathcal{O}(1/r)$ in this expansion, which originates from lowest order FSR-type diagrams. This is the order at which Refs. [1, 5] work. As shown above, in the LO approximation the annihilation cross section proceeds through p -wave. Only higher order terms are able to remove the helicity suppression. We shall further elaborate on this expansion as an operator expansion in Sect. 4.3.

As a check of the results of this subsection, one can use the Ward Identities for EW SM gauge bosons $k_\mu \mathcal{M}_L^\mu \sim 0$, for $m_f \sim 0$, where \mathcal{M}_L^μ is the amplitude computed for the longitudinal mode of the Z . By direct calculation one obtains

$$k_\mu (\mathcal{M}_A^\mu - \mathcal{M}_A^{\mu \text{exc}}) = (\bar{u}_f \gamma_\alpha P_L v_f) \left[\frac{D_{22} - D_{21}}{2} (\bar{v}_\chi \gamma^\alpha u_\chi) + \frac{D_{22} + D_{21}}{2} (\bar{v}_\chi \gamma^\alpha \gamma_5 u_\chi) \right] \quad (4.15)$$

$$k_\mu (\mathcal{M}_C^\mu - \mathcal{M}_C^{\mu \text{exc}}) = -(\bar{u}_f \gamma_\alpha P_L v_f) \left[\frac{D_{11} - D_{12}}{2} (\bar{v}_\chi \gamma^\alpha u_\chi) + \frac{D_{11} + D_{12}}{2} (\bar{v}_\chi \gamma^\alpha \gamma_5 u_\chi) \right] \quad (4.16)$$

$$k_\mu (\mathcal{M}_B^\mu - \mathcal{M}_B^{\mu \text{exc}}) = -(\bar{u}_f \gamma_\alpha P_L v_f) \left[[D_{22} - D_{11} - (D_{21} - D_{12})] (\bar{v}_\chi \gamma^\alpha u_\chi) + [D_{22} - D_{11} + (D_{21} - D_{12})] (\bar{v}_\chi \gamma^\alpha \gamma_5 u_\chi) \right], \quad (4.17)$$

whose vanishing sum confirms the Ward Identity ².

²In the B diagrams, we used the trick $(k_1 - k_2 + p_2 - p_1) \cdot k = D_{11}^{-1} - D_{22}^{-1}$ and $(k_2 - k_1 + p_2 - p_1) \cdot k = D_{12}^{-1} - D_{21}^{-1}$.

It is interesting to see the level of cancellation in the large M_S limit using the properties of Eq. (3.6). We see that, up to order $\mathcal{O}(1/r)$, \mathcal{M}_A and \mathcal{M}_C cancel each other so that, at this order, we can say that their sum is gauge invariant; if we want to keep corrections of order $\mathcal{O}(1/r^2)$ or higher, the full sum of A, C and B diagrams have to be considered in order to have a consistent evaluation

$$k_\mu(\mathcal{M}_A^\mu - \mathcal{M}_A^{\mu\text{exc}} + \mathcal{M}_C^\mu - \mathcal{M}_C^{\mu\text{exc}}) = \mathcal{O}\left(\frac{1}{r^2}\right) + \dots = -k_\mu(\mathcal{M}_B^\mu - \mathcal{M}_B^{\mu\text{exc}}). \quad (4.18)$$

If we do not sum up the full corrections, after summing over the polarizations of the outgoing massive vector, we would end up with unphysical (non-decoupling) $(M_S/m_Z)^2$ and $(M_\chi/m_Z)^2$ corrections [10].

4.2 Results for the cross section

We now turn to evaluate the full 3-body cross section for the process in Eq. (4.1), including VIB diagrams. We follow a rather pedagogical approach, starting from the formula for the cross section

$$d\sigma = \frac{|\mathcal{M}|^2}{4\mathcal{I}} (2\pi)^4 \delta^{(4)}(k_1 + k_2 - p_1 - p_2 - k) \frac{d\mathbf{p}_1}{(2\pi)^3 2p_1^0} \frac{d\mathbf{p}_2}{(2\pi)^3 2p_2^0} \frac{d\mathbf{k}}{(2\pi)^3 2k^0}, \quad (4.19)$$

being $\mathcal{I} = [(k_1 \cdot k_2)^2 - M_\chi^4]^{1/2}$ the initial flux. The squared amplitude $|\mathcal{M}|^2$ is obtained from Eqs. (4.2) and (4.7)-(4.9) by summing over the physical gauge boson polarizations

$$\sum_{i=1,2,3} \epsilon_\mu^i(k) \epsilon_\nu^{i*}(k) = -g_{\mu\nu} + \frac{k_\mu k_\nu}{m_Z^2}. \quad (4.20)$$

Integrating Eq. (4.19) over the three angles that define the position of the plane described through the momentum conservation $\mathbf{p}_1 + \mathbf{p}_2 + \mathbf{k} = 0$ we obtain

$$vd\sigma = \frac{|\mathcal{M}|^2}{1024\pi^4} dx_1 dx_2, \quad (4.21)$$

where x_1 and x_2 parametrize the final energies. In particular, letting $s_1 \equiv (k_1 + k_2)^2$, we have

$$k^0 = (1 - x_2)\sqrt{s_1}/2, \quad (4.22)$$

$$p_1^0 = x_1\sqrt{s_1}/2, \quad (4.23)$$

$$p_2^0 = (1 - x_1 + x_2)\sqrt{s_1}/2, \quad (4.24)$$

and we find the following constraints on the phase space

$$x_- \leq x_1 \leq x_+ \quad \text{with} \quad x_\pm = \frac{1 + x_2}{2} \pm \sqrt{\frac{(1 - x_2)^2}{4} - \frac{m_Z^2}{s_1}} \quad (4.25)$$

$$-\frac{m_Z^2}{s_1} \leq x_2 \leq 1 - 2 \frac{m_Z}{\sqrt{s_1}}. \quad (4.26)$$

The integrations of the squared amplitude over the phase space cannot be carried out exactly, but two limiting situations are of interest: an expansion in powers of $1/r \ll 1$, and the case with $v \rightarrow 0$ with r generic. The results in the former limit are shown below, while the latter case is reported in Appendix B.

Let us parametrize the cross section as

$$v\sigma = \frac{\alpha_W |y_L|^4 (1 - 2s_W^2)^2}{64\pi^2 c_W^2 M_\chi^2} (\rho_s + \rho_p). \quad (4.27)$$

The partially-inclusive cross section, expanded in the large M_S limit ($r \gg 1$), is obtained by integrating Eq. (4.21) over x_1 ; neglecting terms vanishing in the $m_Z \rightarrow 0$ limit we find

$$\begin{aligned} \frac{d\rho_s}{dx_2} &= \frac{4}{3r^4} x_2 (1 - x_2)^3 + \mathcal{O}(r^{-5}), \\ \frac{d\rho_p}{dx_2} &= \frac{v^2}{3r^2} \left[\frac{1 + x_2^2}{1 - x_2} \left(1 - \frac{4}{r} + \frac{11}{r^2} \right) \log \frac{\bar{x}_+}{\bar{x}_-} \right. \\ &\quad \left. + (1 - x_2) \left[2 - \frac{2(x_2 + 5)}{r} + \frac{(-3x_2^3 + 14x_2^2 + 17x_2 + 34)}{r^2} \right] \right] + \mathcal{O}(r^{-5}). \end{aligned} \quad (4.28)$$

with $\bar{x}_\pm = 1 - x_2 \pm \sqrt{(1 - x_2)^2 - \frac{m_Z^2}{M_\chi^2}}$.

The fully-inclusive s -wave and p -wave contributions are obtained by further integrating over x_2 as prescribed in Eq. (4.26); in the large r limit, we get

$$\begin{aligned} \rho_s &= \frac{1}{15r^4} + \mathcal{O}(r^{-5}), \\ \rho_p &= \frac{v^2}{180r^2} \left[60 \left(1 - \frac{4}{r} + \frac{11}{r^2} \right) \ln \frac{2M_\chi}{m_Z} \left(2 \ln \frac{2M_\chi}{m_Z} - 3 \right) \right. \\ &\quad \left. + 10(15 - \pi^2) + \frac{40(\pi^2 - 13)}{r} + \frac{(1059 - 110\pi^2)}{r^2} \right] + \mathcal{O}(r^{-5}). \end{aligned} \quad (4.30)$$

This result shows explicitly the peculiar structure in powers of $1/r$ that we have estimated in Eq. (4.14) using general arguments. As an order-of-magnitude estimate, for velocities $v \sim 10^{-3}$, one expects the 3-body process (in s -wave) to dominate over the 2-body one (in p -wave) for values of $r \lesssim \mathcal{O}(10)$.

Our results are in disagreement with the ones of Ref. [5], where the helicity suppression was removed just by including LO FSR, and where in addition EW corrections proportional to M_χ^2/m_Z^2 were found. Indeed, such terms are present in the physical polarizations sum in Eq. (4.20). However, because of gauge invariance in the form of the Ward Identities written in Eq. (4.18), they disappear from the final result as they should. On the contrary, we find a perfect agreement with the result of Ref. [2] where the photino annihilation process $\tilde{\gamma}\tilde{\gamma} \rightarrow e^+e^-\gamma$ in the $v \rightarrow 0$ limit is analyzed.

4.3 Effective Field Theory Approach

Let us now see how the previous results can be interpreted in the effective field theory language. If the mass of the intermediate scalar particle is much larger than the energy scale

of the non-relativistic annihilation ($E \simeq M_\chi$), then it is possible to integrate the scalar out and perform an operator expansion in the small parameter $1/r = M_\chi^2/M_S^2$. The effective Lagrangian will be given by an infinite series

$$\mathcal{L}_{\text{eff}} = \mathcal{L}_{\text{SM}} + \mathcal{L}_\chi + \frac{1}{r} \frac{\mathcal{O}_6}{M_\chi^2} + \frac{1}{r^2} \frac{\mathcal{O}_8}{M_\chi^4} + \dots, \quad (4.32)$$

where \mathcal{O}_n are dimension- n operators. For the theory we considered in Eq. (2.2), the single dimension-six operator is

$$\mathcal{O}_6 = \frac{1}{2} |y_L|^2 [\bar{\chi} \gamma_\mu \gamma_5 \chi] [\bar{L} \gamma^\mu P_L L], \quad (4.33)$$

which generates the tree level contributions of Eq. (3.5). The corresponding cross section for the $\chi\chi \rightarrow f\bar{f}$ process is

$$v\sigma(\chi\chi \rightarrow f\bar{f})|_{\mathcal{O}_6} = \frac{|y_L|^4}{48\pi M_\chi^2} \frac{v^2}{r^2}, \quad (4.34)$$

where the usual v^2 -suppression appears. Notice that this result can be recovered from Eq. (3.3) in the limit $r \gg 1$ and corresponds to the estimate in Eq. (3.10).

As soon as we add the Z emission (for simplicity we consider only the presence of a single gauge boson Z), at the LO $\mathcal{O}(1/r)$ in the amplitude only the external leg can radiate a gauge boson, making diagrams of the FSR type. We have performed a complete calculation using these effective amplitudes. For the total 3-body cross section we find, neglecting terms vanishing in the limit $m_Z \rightarrow 0$

$$v\sigma(\chi\chi \rightarrow f\bar{f}Z)|_{\mathcal{O}_6} = \frac{\alpha_W |y_L|^4 (1 - 2s_W^2)^2 v^2}{1152\pi^2 c_W^2 M_\chi^2} \frac{v^2}{r^2} \left[15 - \pi^2 + 6 \ln \frac{2M_\chi}{m_Z} \left(2 \ln \frac{2M_\chi}{m_Z} - 3 \right) \right]. \quad (4.35)$$

This expression still bears the v^2 dependence, so that one recovers the result that the EW radiation from the external legs cannot remove the p -wave suppression at LO. Notice that Eq. (4.35) exhibits the usual single and double logarithmic behavior of infrared origin, and that it correctly reproduces the limit for $r \gg 1$ of Eqs. (4.27) and (4.31).

From these results it is clear that limiting the analysis to the dimension-six operator in the effective theory, which corresponds to work in the LO approximation, misses the right result since one could incorrectly conclude that the total cross section itself is p -wave suppressed. As shown in the previous section instead, in order to obtain the correct result, namely that the cross section receives important s -wave contributions, one needs to consider the diagrams (of VIB and FSR type) arising at the next order. Therefore the effect of removing the suppression is encoded by operators of dimension higher than six, for example those in \mathcal{O}_8 .

5 Energy spectra of final stable particles at the interaction point

The analytical results obtained above have a phenomenological impact for DM indirect searches. Indeed, the energy spectra of stable particles produced by DM annihilation, with the inclusion of EW bremsstrahlung, can be very different from those commonly obtained by

working at the LO. In this section we show our results for the energy spectra at the interaction point, focusing in particular on positrons, antiprotons, photons and neutrinos. The propagation of these fluxes of stable particles through the galactic halo will be discussed in Section 6. Our analysis is based on the combination of the analytical description of the primary annihilation channels with the numerical techniques for subsequent hadronization and decay. Let us now describe our procedure in more detail.

As already discussed, we work in the approximation of massless external fermions, under which the calculations of the previous sections have been performed. So we consider only the case where $L = (\nu_{eL}, e_L)$, for which this is an excellent approximation. In general, channels with external fermions of mass m_f would receive other, different contributions proportional to $(m_f/M_\chi)^2$, in addition to the s -wave contribution from VIB and FSR, as discussed at length above. The primary annihilation channels for $\chi\chi \rightarrow I$, including EW bremsstrahlung, are

$$I = \{e_L^+ e_L^-, \nu_{eL} \bar{\nu}_{eL}, e_L^+ e_L^- \gamma, e_L^+ \nu_{eL} W^-, e_L^- \bar{\nu}_{eL} W^+, e_L^+ e_L^- Z, \nu_{eL} \bar{\nu}_{eL} Z\}. \quad (5.1)$$

The different 3-body channels are simply related by different gauge couplings

$$\sigma(\chi\chi \rightarrow \nu_{eL} \bar{\nu}_{eL} Z) = \frac{1}{(1 - 2s_W^2)^2} \sigma(\chi\chi \rightarrow e_L^+ e_L^- Z), \quad (5.2)$$

$$\sigma(\chi\chi \rightarrow e_L^- \bar{\nu}_{eL} W^+) = \sigma(\chi\chi \rightarrow e_L^+ \nu_{eL} W^-) = \frac{2c_W^2}{(1 - 2s_W^2)^2} \sigma(\chi\chi \rightarrow e_L^+ e_L^- Z)|_{m_Z \rightarrow m_W} \quad (5.3)$$

$$\sigma(\chi\chi \rightarrow e_L^+ e_L^- \gamma) = \frac{4c_W^2 s_W^2}{(1 - 2s_W^2)^2} \sigma(\chi\chi \rightarrow e_L^+ e_L^- Z)|_{m_Z \rightarrow 0}. \quad (5.4)$$

We have written our own Monte Carlo code to generate parton-level events for DM annihilations into 2- and 3-body final states, in the frame where the total spatial momentum is zero. While for the $2 \rightarrow 2$ processes the final state consists of two back-to-back particles, the 3-body final states require particular care because the probability distribution of the momenta of the outgoing particles is dictated by the double-differential probability distributions

$$\frac{1}{\sigma(\chi\chi \rightarrow 3\text{-body})} \frac{d\sigma(\chi\chi \rightarrow 3\text{-body})}{dx_1 dx_2}, \quad (5.5)$$

where x_1 and x_2 are related to the energy fractions of the outgoing particles, as in Eqs. (4.22), (4.23), (4.24).

A large number of events (2×10^5) for each annihilation channel in Eq. (5.1) is generated in this way, and then passed through PYTHIA 8.145 [11] for simulating the subsequent showering, hadronization and decay³. All unstable particles are requested to decay so that the only final particles remaining in the sample are the stable species of the SM. We have performed several checks at various levels to assess the reliability of our numerical code. For instance, we have found excellent agreement with the results of Ref. [1].

³PYTHIA 8.1 has been preferred over the predecessor PYTHIA 6.4 because of the inclusion of the photon branchings into fermion-antifermion in the showering process.

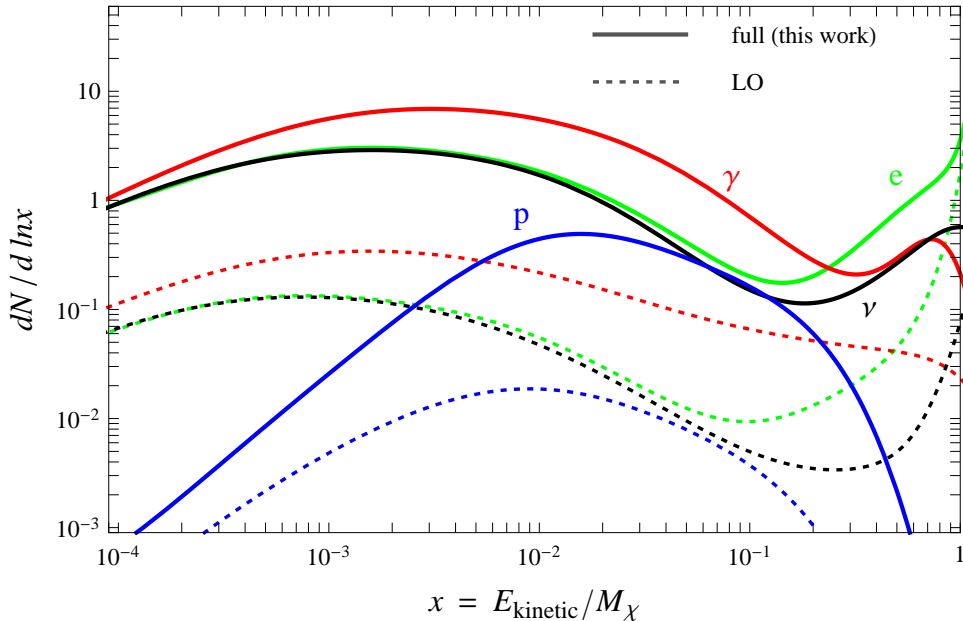


Figure 3: The spectra $d\mathcal{N}_f/d\ln x$, as defined in Eq. (5.6), for e^+ (green), γ (red), $\nu = (\nu_e + \nu_\mu + \nu_\tau)/3$ (black) and \bar{p} (blue), from the annihilation $\chi\chi \rightarrow e_L^+ e_L^-, \nu_{eL} \bar{\nu}_{eL}$ with the corresponding weak boson emission corrections, for the case $M_\chi = 1 \text{ TeV}$, $M_S = 4 \text{ TeV}$, $v = 10^{-3}$ (solid lines). For comparison, we show the spectra (dashed lines) in the LO approximation (see text for details).

Fitting the numerical results, it is possible to extract the energy distributions of each stable particle f

$$\frac{d\mathcal{N}_f}{d\ln x} \equiv \frac{1}{\sigma_0} \frac{d\sigma(\chi\chi \rightarrow f + X)}{d\ln x}, \quad f = \{e^+, e^-, \gamma, \nu, \bar{\nu}, p, \bar{p}\}, \quad (5.6)$$

where $x \equiv E_{\text{kinetic}}^{(f)}/M_\chi$, $E_{\text{kinetic}}^{(f)}$ is the kinetic energy of the particle f (the difference between total and kinetic energies is obviously relevant only for the (anti)protons), and the X reminds us of the inclusivity in the final state with respect to the particle f . As a normalization, we have chosen the tree-level cross section of the 2-body processes ⁴

$$\sigma_0 = \sigma_{\text{tree}}(\chi\chi \rightarrow e_L^+ e_L^-) + \sigma_{\text{tree}}(\chi\chi \rightarrow \nu_{eL} \bar{\nu}_{eL}). \quad (5.7)$$

The plot in Figure 3 shows the resulting $d\mathcal{N}_f/dx$ for $e^+, \gamma, \nu = (\nu_e + \nu_\mu + \nu_\tau)/3, \bar{p}$ for a specific, but representative, choice of parameters: $M_\chi = 1 \text{ TeV}$, $M_S = 4 \text{ TeV}$ (corresponding

⁴ Another choice for the normalization would be the total cross section $\sigma(\chi\chi \rightarrow f + X)$, which would provide the quantity in Eq. (5.6) with a more transparent physical interpretation as the energy spectrum of f . However, $\sigma(\chi\chi \rightarrow f + X)$ is not as easily calculable as the 2-body cross section and it would not be possible to compare the energy spectra with and without the s -wave contributions because their total cross sections would be different. In any case, the specific choice of the normalization becomes irrelevant when taking ratios of spectra, which serve to stress the relevance of the effect we are studying.

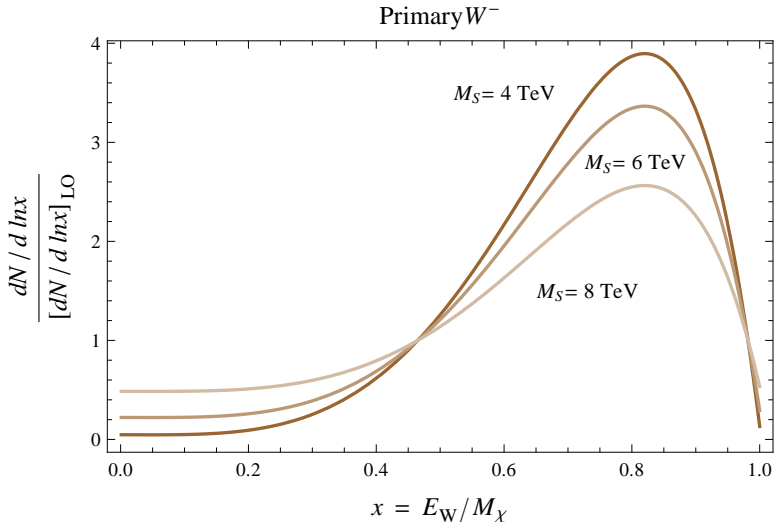


Figure 4: Ratios between the energy spectrum of the W^- gauge boson in the 3-body annihilation channel $\chi\chi \rightarrow e_L^+ \nu_e W^-$ for different values of M_S with respect to the same energy spectrum computed in the LO approximation (see text for details).

to $r = 16$) and $v = 10^{-3}$; for comparison, the situation where only the LO term is taken into account is also shown (recall that what LO means has been discussed in Sect. 4.1). The energy spectra result to be much larger than those obtained in the LO approximation. This is a consequence of having a sizeable s -wave annihilation channel opened at the next-to-leading order in the $1/r$ expansion. To better clarify this point we remind that – as already discussed in Ref. [1] – the emission of an EW gauge boson opens the hadronic channel, and has dramatic consequences on the final state: antiprotons as well as a large number of soft photons, positrons and neutrinos from pion decays are produced leading to a huge enhancement in the low-energy tail of the energy spectra of final stable particles. The situation described in Ref. [1] is obtained here in correspondence of the LO approximation where – as discussed in Section 4 – the p -wave term in the 3-body cross section dominates widely over the s -wave one, giving corrections factorized with respect to the tree-level annihilation process. Going beyond the LO, the opening of a sizeable s -wave contribution results into a harder energy spectrum for the primary gauge boson which is entirely converted (after decay and hadronization processes) into low energy stable particles, thus leading to a greater enhancement in the low-energy tails of their spectra.

An interesting spectral feature of the gamma rays originates from the inclusion of EW corrections (see Figure 3). Indeed, the gamma ray spectrum is the composition of a bump in the hard region due to the contribution of hard photons coming from the s -wave in the primary annihilation channel $\chi\chi \rightarrow e_L^+ e_L^- \gamma$, and a huge tail of soft ones originating from showering processes and from the hadronization of the W and Z gauge bosons included in our analysis.

The relevance of the effect of removing the suppression is made more manifest by taking the ratios between the energy spectra computed at given M_S with respect to those obtained in the

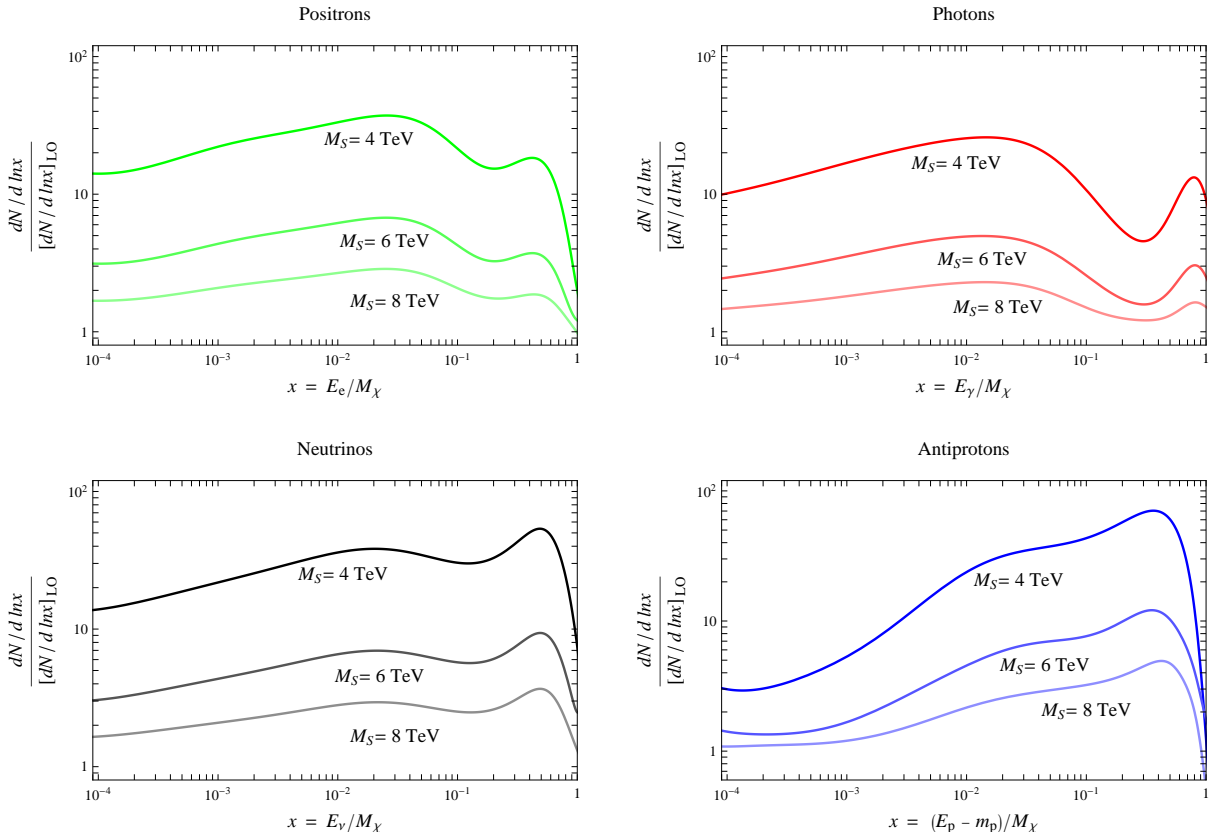


Figure 5: Ratios between the energy spectra of final stable particles for different values of M_S with respect to those computed in the LO approximation (see text for details).

LO approximation, as shown in Figure 4 and in Figure 5, for different values of M_S . In Figure 4 we plot these ratios before hadronization and decays, considering as example the spectrum of the primary W^- gauge boson in the 3-body annihilation channel $\chi\chi \rightarrow e_L^+ \nu_{eL} W^-$. The growth in the hard region as the s -wave contribution becomes larger is apparent; this prerogative is present in all the 3-body channels included in our analysis and listed in Eq. (5.1). In Figure 5, we show the ratios of the energy spectra of the final stable particles after hadronization and decays, with respect to those at LO. The impact of the EW radiation beyond LO can result into an enhancement of the energy spectra even by factors $\mathcal{O}(10 - 100)$.

6 Fluxes of final stable particles at detection

The previous sections have focused on the calculations of the energy spectra of stable SM particles at the interaction point, normalized for each DM annihilation event. In this section we want to make contact with the phenomenological observables and thus compute the fluxes of electrons, positrons, antiprotons, prompt gamma rays and neutrinos that can be measured at Earth. We first recall briefly the basics of the computation of such fluxes (see e.g. Ref. [12] for a lucid and pedagogical review) and then illustrate the results for the energy spectra found in the previous section.

6.1 Basics of galactic propagation of stable particles

Dark Matter distribution in the galactic halo. The DM density profile in the galactic halo, $\rho(\vec{x})$, is one of the essential ingredients to determine the normalization of the fluxes of cosmic rays that are collected at Earth. N-body numerical simulations performed in the latest decades have found different answers for $\rho(r)$. While recent simulations seem to individuate the Einasto profile as the best option, the Navarro-Frenk-White (NFW) profile is still widely used in the literature and the cored Burkert profile (disfavored by simulations) is sometimes advocated as a better fit to astronomical observations. These profiles explicitly read

	$\rho(r)$	r_s [kpc]	ρ_s [GeV/cm ³]
NFW [13]	$\rho_s \frac{r_s}{r} \left(1 + \frac{r}{r_s}\right)^{-2}$	24.42	0.184
Einasto [14]	$\rho_s \exp \left[-\frac{2}{0.17} \left[\left(\frac{r}{r_s}\right)^{0.17} - 1 \right] \right]$	28.44	0.033
Burkert [15]	$\frac{\rho_s}{(1 + r/r_s)(1 + (r/r_s)^2)}$	12.7	0.712

where, in order to fix the parameters r_s and ρ_s at their precise values, one imposes the constraints that ρ_\odot (the value of the DM density at the location of the solar system) = 0.3 GeV/cm³ and that the total DM mass contained in the Milky Way reproduces observations (see Ref. [16]). They differ most at the Galactic Center (GC): NFW is peaked as r^{-1} while Burkert is constant in the inner 1 kpc. They are instead similar around the location of the solar system, due also to the ρ_\odot constraint. As long as a convergent determination of the actual DM profile is not reached, it is sensible to have at disposal the whole range of these possible choices when computing Dark Matter signals in the Milky Way. In other words, the ignorance on the actual DM profile constitutes a (currently) irreducible astrophysical uncertainty for the predicted fluxes.

Charged particles (electrons, positrons, antiprotons). The e^- , e^+ and \bar{p} produced in any given point of the halo propagate immersed in the turbulent galactic magnetic field. The field consists of random inhomogeneities that act as scattering centers for charged particles, so that their journey can effectively be described as a diffusion process from an extended source (the DM halo) to some final given point (the location of the Earth, in the case of interest). The number density $n_f(\vec{x}, E)$ per unit energy E of the cosmic ray species f ($= e^+, e^-, \bar{p}$) in any given point \vec{x} evolves according to a diffusion-loss equation [12]

$$-\mathcal{K}(E) \cdot \nabla^2 n_f - \frac{\partial}{\partial E} (b(E, \vec{x}) n_f) + \frac{\partial}{\partial z} (\text{sign}(z) V_{\text{conv}} n_f) = Q(E, \vec{x}) - 2h \delta(z) \Gamma n_f. \quad (6.1)$$

The first term accounts for diffusion, with a coefficient conventionally parameterized as $\mathcal{K}(E) = \mathcal{K}_0 (E/\text{GeV})^\delta$. The second term describes energy losses: the coefficient b is position-dependent since the intensity of the magnetic field (which determines losses due to synchrotron radiation) and the distribution of the photon field (which determines losses due to inverse Compton scattering) vary across the galactic halo. The third term deals with convection

while the last term accounts for nuclear spallations, that occur with rate Γ in the disk of thickness $h \simeq 100$ pc. The source, DM annihilations, is denoted by Q . The different processes described above have a different importance depending on the particle species: the journey of electrons and positrons is primarily affected by synchrotron radiation and inverse Compton energy losses, while for antiprotons these losses are negligible and convection and spallation dominate.

Eq. (6.1) is usually solved numerically in a diffusive region with the shape of a solid flat cylinder that sandwiches the galactic plane, with height $2L$ in the z direction and radius $R = 20$ kpc in the r direction. The location of the solar system corresponds to $\vec{x}_\odot = (r_\odot, z_\odot) = (8.33 \text{ kpc}, 0)$. Boundary conditions are imposed such that the number density n_f vanishes on the surface of the cylinder, outside of which the charged cosmic rays freely propagate and escape. The values of the propagation parameters δ , K_0 , V_{conv} and L are deduced from a variety of (ordinary) cosmic ray data and modelizations. It is customary to adopt the following sets, denoted with MIN, MED and MAX because they are found to minimize or maximize the final fluxes

Model	Electrons or positrons		Antiprotons			L [kpc]
	δ	\mathcal{K}_0 [kpc ² /Myr]	δ	\mathcal{K}_0 [kpc ² /Myr]	V_{conv} [km/s]	
MIN	0.55	0.00595	0.85	0.0016	13.5	1
MED	0.70	0.0112	0.70	0.0112	12	4
MAX	0.46	0.0765	0.46	0.0765	5	15

As long as independent measurements do not allow to pin down more precisely the values of these parameters, the scatter among such different sets constitute an additional astrophysical uncertainty on the predicted DM fluxes, this time due to the propagation process.

The solution of Eq. (6.1) allows to compute the phenomenological quantity in which we are interested: the flux of cosmic rays received at Earth $d\Phi_f/dE = v_f n_f/4\pi$ (where v_f is the velocity of species f , equal to c for e^\pm but possibly different for mildly-relativistic \bar{p}). It turns out that, both for e^\pm and for \bar{p} , the flux can be conveniently expressed as a convolution of the spectra at the interaction point with some universal functions that encapsulate the astrophysics of the ‘production and propagation’ process. More precisely, for e^\pm one has

$$\frac{d\Phi_{e^\pm}}{dE}(E, \vec{x}_\odot) = \frac{v_{e^\pm}}{4\pi b(E, \vec{x}_\odot)} \frac{1}{2} \left(\frac{\rho_\odot}{M_\chi} \right)^2 \langle \sigma v \rangle \int_E^{M_\chi} dE_s \frac{dN_{e^\pm}}{dE}(E_s) I(E, E_s, \vec{x}_\odot), \quad (6.2)$$

where dN_{e^\pm}/dE are the spectra at the annihilation point and $I(E, E_s, \vec{x}_\odot)$ are (generalized) halo functions which are independent of the particle physics model: there is such a function for each choice of DM distribution profile and choice of e^\pm propagation parameters. We are following here the formalism discussed in Ref. [16], which allows in particular to take into account the spatial dependence of the energy loss coefficient b for e^\pm discussed above. We refer to Ref. [16] for all details, including an explicit form of b and of the I functions, and further references. Similarly, for \bar{p} one has

$$\frac{d\Phi_{\bar{p}}}{dE}(E, \vec{x}_\odot) = \frac{v_{\bar{p}}}{4\pi} \left(\frac{\rho_\odot}{M_\chi} \right)^2 R(E) \frac{1}{2} \langle \sigma v \rangle \frac{dN_{\bar{p}}}{dE}. \quad (6.3)$$

where it is now the function $R(E)$ which contains the astrophysics: again, there is such a function for each choice of DM distribution profile and the choice of \bar{p} propagation parameters.

Neutral particles (photons, neutrinos). Neutral messengers produced by DM annihilation in any given point of the DM halo travel along a straight line to the Earth. Since absorption in the Galaxy is negligible, the flux from a given direction is the result of the contribution from all the Dark Matter intervening along the line of sight. The integrated flux of gamma rays or neutrinos over a region $\Delta\Omega$, corresponding e.g. to the window of observation or the resolution of the telescope, is given by

$$\frac{d\Phi_{\gamma,\nu}}{dE}(E) = \frac{r_\odot}{4\pi} \frac{1}{2} \left(\frac{\rho_\odot}{M_\chi} \right)^2 \bar{J} \Delta\Omega \langle\sigma v\rangle \frac{dN_{\gamma,\nu}}{dE}, \quad \text{with } \bar{J} = \frac{1}{\Delta\Omega} \int_{\Delta\Omega} \int_{\text{l.o.s.}} \frac{ds}{r_\odot} \left(\frac{\rho(r(s,\theta))}{\rho_\odot} \right)^2, \quad (6.4)$$

where $dN_{\gamma,\nu}/dE$ denotes as usual the spectra at the annihilation point and the average J factor contains the integral along the line of sight (l.o.s.). Here the coordinate r , centered on the GC, reads $r(s, \theta) = (r_\odot^2 + s^2 - 2r_\odot s \cos\theta)^{1/2}$: s runs along the l.o.s. and θ is the aperture angle between the direction of the l.o.s. and the axis connecting the Earth to the GC. For a fixed window $\Delta\Omega$, the value of \bar{J} can span orders of magnitude depending on the choice of the DM profile, especially if the window is small and close to the region where the profiles differ most, i.e. the GC. We refer to Ref. [16] for some explicit values of \bar{J} in selected windows.

6.2 Results

In Figure 6 we show the fluxes of charged cosmic rays for the representative choice of model parameters already used in Section 5 (namely, $M_\chi = 1$ TeV and $M_S = 4$ TeV). We do not adopt here a specific value for the annihilation cross section $\langle\sigma v\rangle$, which obviously enters as a normalizing constant in Eqs. (6.2) and (6.3): in the context of the toy model that we are considering, its value is very small, if one requires the cosmological relic abundance of this DM candidate to be fixed by the thermal freeze-out mechanism. This is not surprising and it is actually the typical case for Bino-like Dark Matter in supersymmetry. Notice that if one adopts the normalization with the 2-body annihilations, as done in Sect. 5, the energy spectra and the cross section appearing in the expressions for the fluxes should be replaced by the analogous quantities in Eqs. (5.6) and (5.7). What we are more interested in is verifying that the enhancement of the fluxes remains significant on the phenomenological observables (the spectra after propagation) and distinct from the normalization issues due to the propagation itself. This is indeed the case, as Figure 6 shows. In these plots, the solid lines represent the fluxes computed with ‘NFW’ as the choice of DM profile and with ‘MED’ propagation parameters. The shaded bands show the variance of this prediction that one obtains by making other choices. The bands span quite a large area since both the DM profile and the propagation parameters are varied simultaneously.

The fluxes of e^\pm and \bar{p} are about one order of magnitude higher than those computed in the LO approximation, consistently with what expected from input fluxes, and emerge quite clearly from the uncertainty bands, especially for electrons or positrons at high energies. Small

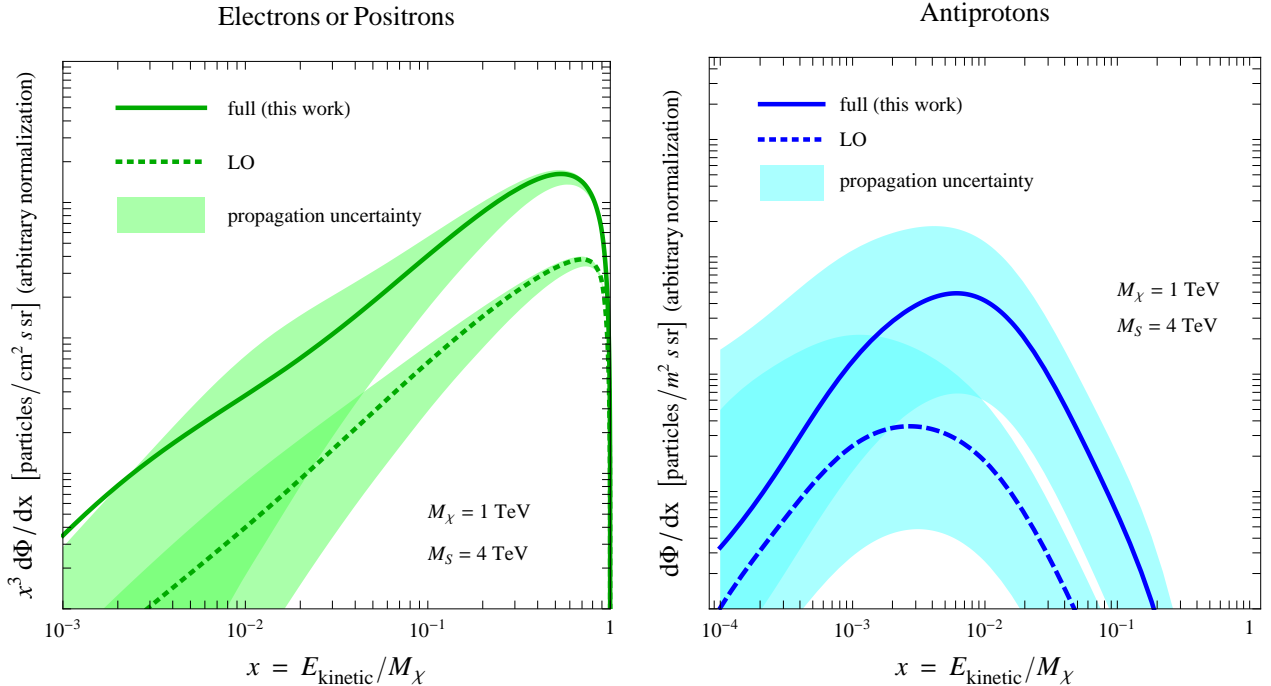


Figure 6: Fluxes of electrons or positrons (left panel) and of antiprotons (right panel) after propagation in the galactic halo.

differences in the shapes of the spectra, that were marginally visible in the input spectra, see Figure 3, are essentially washed out for electrons and positrons (since the energy losses tend to smooth any spectral feature) but remain somewhat discernible in the antiproton spectrum (since propagation does not significantly reshuffle energies for this species).

In the case of neutral particles (gamma rays and neutrinos), the fluxes ‘at detection’ are easily computed with the use of Eq. (6.4). They simply correspond to a re-normalization of the input fluxes, for a given choice of the observational window and the DM profile (which fixes the \bar{J} factor), so that we do not plot them explicitly. Any peculiar spectral feature possibly introduced by contributions beyond the LO approximation, e.g. the high-energy bump discussed above in the gamma ray spectrum, would of course be conserved.

7 Summary and conclusions

We have investigated the relevance of the EW corrections in theories where the cross section for DM annihilation into 2-body final states is suppressed. A Majorana DM annihilating into two light SM fermions is one such case. We have worked for simplicity with a model where the DM is a Majorana fermion of mass M_χ and a SM singlet, which annihilates into SM fermions through the exchange of a heavy scalar doublet of mass M_S , and carried out an expansion in $1/r \equiv (M_\chi/M_S)^2 \ll 1$.

Let us summarize our main results:

- at the lowest order ($1/r$ in the amplitude) the radiation of EW gauge bosons is not able to remove the helicity suppression and the process stays in the p -wave (see Eq. (3.10) for an estimate and Eq. (3.3) for the precise result);
- an efficient removal of the suppression, opening up a potentially large s -wave, is achieved by including EW radiation at the next-to-leading order ($1/r^2$ in the amplitude), which comes from both FSR and VIB diagrams (see Eq. (4.14) for an estimate and Eqs. (4.30)-(4.31) for the precise result);
- the resulting energy spectra of stable particles, in the annihilation region, get substantially enhanced by this effect by factors $\mathcal{O}(10 - 100)$ (see Figure 5).

Furthermore, such an effect does not get spoiled by galactic propagation and crucially affects the predictions for fluxes to be measured at Earth (see Figure 6).

We have also interpreted our findings in the language of effective field theory and pointed out that the effect of opening up the s -wave is missed by dimension-six operators and only caught by higher-dimensional operators. This is an example where the naive dimensional power counting fails to assess the relative importance of the operators in the expansion, as far as the EW radiation is concerned.

Our results have a wider generality than the specific model we have considered. Reliable computations of energy spectra of stable particles and predictions for their fluxes at Earth – the key observable for DM indirect searches – cannot prescind from including the effects of EW radiation.

Acknowledgments

We are grateful to Stephen Mrenna, Torbjörn Sjöstrand, and Peter Skands for useful correspondence about PYTHIA, and to Paolo Torrielli for helpful advices on numerical issues. The work of ADS is supported by the Swiss National Science Foundation under contract 200021-125237. The work of AU is supported by CICYT-FEDER-FPA2008-01430.

A The Dirac case

We list here the analogous results of Sections 3 and 4 for the case of Dirac Dark Matter.

The 2-body annihilation cross section into a pair of massless left-handed fermions is

$$v\sigma = a + b v^2 + \mathcal{O}(v^4), \quad (\text{A.1})$$

where

$$a = \frac{|y_L|^4}{32\pi(1+r)^2 M_\chi^2}, \quad b = \frac{|y_L|^4(r^2 - 3r - 1)}{96\pi M_\chi^2(1+r)^4}. \quad (\text{A.2})$$

For the process in Eq. (4.1), the exchanged diagrams of Figure 2 are absent and the amplitude can be written as

$$i\mathcal{M} \cdot \epsilon^* = \frac{ig|y_L|^2(1-2s_W^2)}{4c_W} [\mathcal{M}_A + \mathcal{M}_B + \mathcal{M}_C], \quad (\text{A.3})$$

and by using the Fierz transformation (4.4) the three terms analog of Eqs. (4.7)-(4.9) become

$$\mathcal{M}_A = \frac{\bar{u}_f \not{\epsilon}^*(k) (\not{p}_1 + \not{k}) P_R \gamma^\mu v_f}{2p_1 \cdot k + m_Z^2} \cdot \left(\frac{D_{22}}{2} \bar{v}_\chi \gamma_\mu u_\chi + \frac{D_{22}}{2} \bar{v}_\chi \gamma_\mu \gamma_5 u_\chi \right), \quad (\text{A.4})$$

$$\mathcal{M}_B = (-1) [\bar{u}_f P_R \gamma^\mu v_f] [(k_1 - k_2 - p_1 + p_2) \cdot \epsilon^*(k) \bar{v}_\chi P_L \gamma_\mu u_\chi D_{11} D_{22}] \quad (\text{A.5})$$

$$\mathcal{M}_C = -\frac{\bar{u}_f P_R \gamma^\mu (\not{p}_2 + \not{k}) \not{\epsilon}^*(k) v_f}{2p_2 \cdot k + m_Z^2} \cdot \left(\frac{D_{11}}{2} \bar{v}_\chi \gamma_\mu u_\chi + \frac{D_{11}}{2} \bar{v}_\chi \gamma_\mu \gamma_5 u_\chi \right). \quad (\text{A.6})$$

Then the calculation of the cross sections proceeds as described in Section 4.2 and we choose the parametrization in terms of ρ_s and ρ_p as in Eq. (4.27). In particular for the partially-inclusive cross section in the large M_S limit we find, neglecting terms vanishing in the $m_Z \rightarrow 0$ limit

$$\begin{aligned} \frac{d\rho_s}{dx_2} &= \frac{1}{6r^2} \left[(1-x_2) \left[-6 + \frac{6(x_2+3)}{r} + \frac{(4x_2^3 - 26x_2^2 - 26x_2 - 30)}{r^2} \right] \right. \\ &\quad \left. + \frac{1+x_2^2}{1-x_2} \left(3 - \frac{6}{r} + \frac{9}{r^2} \right) \ln \frac{\bar{x}_+}{\bar{x}_-} \right] + \mathcal{O}(r^{-5}), \end{aligned} \quad (\text{A.7})$$

$$\begin{aligned} \frac{d\rho_p}{dx_2} &= \frac{v^2}{36r^2} \left[(1-x_2) \left[-12 + \frac{3(7x_2+35)}{r} + \frac{(18x_2^3 - 137x_2^2 - 227x_2 - 392)}{r^2} \right] \right. \\ &\quad \left. + \frac{6(1+x_2^2)}{1-x_2} \left(1 - \frac{7}{r} + \frac{21}{r^2} \right) \ln \frac{\bar{x}_+}{\bar{x}_-} \right] + \mathcal{O}(r^{-5}). \end{aligned} \quad (\text{A.8})$$

For completeness, we also evaluate the expressions for the fully-inclusive s -wave and p -wave contributions

$$\begin{aligned} \rho_s &= \frac{1}{60r^2} \left[30 \left(1 - \frac{2}{r} + \frac{3}{r^2} \right) \ln \frac{2M_\chi}{m_Z} \left(2 \ln \frac{2M_\chi}{m_Z} - 3 \right) \right. \\ &\quad \left. + 5(\pi^2 - 15) - \frac{10(\pi^2 - 11)}{r} + \frac{3(5\pi^2 - 34)}{r^2} \right], \end{aligned} \quad (\text{A.9})$$

$$\begin{aligned} \rho_p &= \frac{v^2}{360r^2} \left[30 \ln \frac{2M_\chi}{m_Z} \left[4 \left(1 - \frac{7}{r} + \frac{21}{r^2} \right) \ln \frac{2M_\chi}{m_Z} - 3 \left(1 - \frac{12}{r} + \frac{39}{r^2} \right) \right] \right. \\ &\quad \left. + \frac{5}{2}(33 - 4\pi^2) + \frac{5(14\pi^2 - 155)}{r} + \frac{42(42 - 5\pi^2)}{r^2} \right]. \end{aligned} \quad (\text{A.10})$$

B 3-body cross section in the $v \rightarrow 0$ limit

We report here the results for the cross section of the 3-body process $\chi\chi \rightarrow f\bar{f}Z$, in the limit $v \rightarrow 0$, therefore retaining only the part of the process proceeding through the s -wave. We

do not expand in powers of $1/r$, so the following results are valid for any value of $r \geq 1$. The cross section is parametrized as in Eq. (4.27)

$$v\sigma|_{v \rightarrow 0} = \frac{\alpha_W |y_L|^4 (1 - 2s_W^2)^2}{64\pi^2 c_W^2 M_\chi^2} \rho_s^{(v=0)}. \quad (\text{B.1})$$

The partially-inclusive contribution to the differential cross section is

$$\begin{aligned} \frac{d\rho_s^{(v=0)}}{dx_2} &= \frac{\frac{m_Z^2}{4M_\chi^2} + x_2}{(r + x_2)^2} \left[\frac{\frac{m_Z^2}{M_\chi^2} + 2x_2(r + 1) + r^2 - 1}{4(r + x_2)} \log \left[\frac{r + x_2 - \bar{y}}{r + x_2 + \bar{y}} \right] \right. \\ &\quad \left. - \frac{\bar{y} \frac{m_Z^2}{M_\chi^2} - 2x_2(r + x_2 - 1) - r^2 - 1}{2 \frac{m_Z^2}{M_\chi^2} + 2x_2(r + 1) + r^2 - 1} \right], \end{aligned} \quad (\text{B.2})$$

with $\bar{y} = \sqrt{(1 - x_2)^2 - \frac{m_Z^2}{M_\chi^2}}$. The fully-inclusive cross section is obtained by integrating the previous expressions over the kinematical domain in Eq. (4.26). Neglecting terms vanishing in the limit $m_Z \rightarrow 0$ we find

$$\rho_s^{(v=0)} = \frac{1}{4r(1+r)} [A(r)r^3 + B(r)r^2 + C(r)r + D(r)], \quad (\text{B.3})$$

where

$$\begin{aligned} A(r) &= \text{Li}_2\left(\frac{r-1}{2r}\right) - \text{Li}_2\left(\frac{r+1}{2r}\right) + \ln(r+1) \ln \frac{r}{r^2-1} \\ &\quad + \ln(r-1) \ln \frac{(r+1)^2}{r} + (\ln 2 - 2) \ln \frac{r+1}{r-1}, \end{aligned} \quad (\text{B.4})$$

$$B(r) = 2 \left[\text{Li}_2\left(\frac{r-1}{2r}\right) - \text{Li}_2\left(\frac{r+1}{2r}\right) + \left(\ln \frac{r}{r+1} + \ln 2 - \frac{1}{4} \right) \ln \frac{r+1}{r-1} + 2 \right], \quad (\text{B.5})$$

$$C(r) = \text{Li}_2\left(\frac{r-1}{2r}\right) - \text{Li}_2\left(\frac{r+1}{2r}\right) + \left(\ln \frac{r}{r+1} + \ln 2 + 2 \right) \ln \frac{r+1}{r-1} + 3, \quad (\text{B.6})$$

$$D(r) = \frac{1}{2} \ln \frac{r+1}{r-1}, \quad (\text{B.7})$$

being $\text{Li}_2(z) \equiv \sum_{k=1}^{\infty} z^k/k^2$ the usual dilogarithm.

References

- [1] P. Ciafaloni, D. Comelli, A. Riotto, F. Sala, A. Strumia and A. Urbano, *Weak Corrections are Relevant for Dark Matter Indirect Detection*, JCAP **1103**, 019 (2011), [arXiv:1009.0224](https://arxiv.org/abs/1009.0224).
- [2] L. Bergstrom, *Radiative Processes in Dark Matter Photino Annihilation*, Phys. Lett. B **225** (1989) 372.

- [3] T. Bringmann, L. Bergstrom and J. Edsjo, *New Gamma-Ray Contributions to Supersymmetric Dark Matter Annihilation*, JHEP **0801** (2008) 049, [arXiv:0710.3169](#).
- [4] L. Bergstrom, T. Bringmann and J. Edsjo, *New Positron Spectral Features from Supersymmetric Dark Matter - a Way to Explain the PAMELA Data?*, Phys. Rev. D **78** (2008) 103520, [arXiv:0808.3725](#).
- [5] N. F. Bell, J. B. Dent, T. D. Jacques and T. J. Weiler, *W/Z Bremsstrahlung as the Dominant Annihilation Channel for Dark Matter*, Phys. Rev. D **83**, 013001 (2011), [arXiv:1009.2584](#); N. F. Bell, J. B. Dent, T. D. Jacques and T. J. Weiler, *Dark Matter Annihilation Signatures from Electroweak Bremsstrahlung*, [arXiv:1101.3357](#).
- [6] V. Berezhinsky, M. Kachelriess and S. Ostapchenko, *Electroweak jet cascading in the decay of superheavy particles*, Phys. Rev. Lett. **89** (2002) 171802, [arXiv:hep-ph/0205218](#); C. Barbot and M. Drees, *Production of ultraenergetic cosmic rays through the decay of superheavy X particles*, Phys. Lett. B **533** (2002) 107, [arXiv:hep-ph/0202072](#); C. Barbot and M. Drees, *Detailed analysis of the decay spectrum of a super heavy X particle*, Astropart. Phys. **20** (2003) 5, [arXiv:hep-ph/0211406](#); M. Kachelriess and P. D. Serpico, *Model-independent dark matter annihilation bound from the diffuse γ ray flux*, Phys. Rev. D **76** (2007) 063516, [arXiv:0707.0209](#); N. F. Bell, J. B. Dent, T. D. Jacques and T. J. Weiler, *Electroweak Bremsstrahlung in Dark Matter Annihilation*, Phys. Rev. D **78** (2008) 083540, [arXiv:0805.3423](#); J. B. Dent, R. J. Scherrer and T. J. Weiler, *Toward a Minimum Branching Fraction for Dark Matter Annihilation into Electromagnetic Final States*, Phys. Rev. D **78** (2008) 063509 [arXiv:0806.0370](#); V. Barger, Y. Gao, W. Y. Keung, D. Marfatia, *Generic dark matter signature for gamma-ray telescopes*, Phys. Rev. **D80** (2009) 063537, [arXiv:0906.3009](#); J. F. Fortin, J. Shelton, S. Thomas and Y. Zhao, *Gamma Ray Spectra from Dark Matter Annihilation and Decay*, [arXiv:0908.2258](#); M. Kachelriess, P. D. Serpico and M. A. Solberg, *“On the role of electroweak bremsstrahlung for indirect dark matter signatures*, Phys. Rev. D **80** (2009) 123533, [arXiv:0911.0001](#).
- [7] X. -l. Chen, M. Kamionkowski, *Three body annihilation of neutralinos below two-body thresholds*, JHEP **9807** (1998) 001, [hep-ph/9805383](#); C. E. Yaguna, *Large contributions to dark matter annihilation from three-body final states*, Phys. Rev. **D81** (2010) 075024, [arXiv:1003.2730](#); K. -Y. Choi, D. Restrepo, C. E. Yaguna, O. Zapata, *Indirect detection of gravitino dark matter including its three-body decays*, JCAP **1010** (2010) 033, [arXiv:1007.1728](#);
- [8] See for instance, M. Beltran, D. Hooper, E. W. Kolb and Z. C. Krusberg, *Deducing the nature of dark matter from direct and indirect detection experiments in the absence of collider signatures of new physics*, Phys. Rev. D **80**, 043509 (2009), [arXiv:0808.3384](#); R. Harnik and G. D. Kribs, *An Effective Theory of Dirac Dark Matter*, Phys. Rev. D **79**, 095007 (2009), [arXiv:0810.5557](#); M. Berg, J. Edsjo, P. Gondolo, E. Lundstrom and S. Sjons, *Neutralino Dark Matter in BMSSM Effective Theory*, JCAP **0908**, 035 (2009),

- [arXiv:0906.0583](#); Q. H. Cao, C. R. Chen, C. S. Li and H. Zhang, *Effective Dark Matter Model: Relic density, CDMS II, Fermi LAT and LHC*, [arXiv:0912.4511](#); J. Fan, M. Reece and L. T. Wang, *Non-relativistic effective theory of dark matter direct detection*, JCAP **1011**, 042 (2010), [arXiv:1008.1591](#); J. Goodman, M. Ibe, A. Rajaraman, W. Shepherd, T. M. P. Tait and H. B. P. Yu, *Gamma Ray Line Constraints on Effective Theories of Dark Matter*, Nucl. Phys. B **844**, 55 (2011), [arXiv:1009.0008](#); K. Cheung, P. Y. Tseng and T. C. Yuan, *Cosmic Antiproton Constraints on Effective Interactions of the Dark Matter*, JCAP **1101**, 004 (2011), [arXiv:1011.2310](#); E. Del Nobile and F. Sannino, *Dark Matter Effective Theory*, [arXiv:1102.3116](#).
- [9] E. Ma, *Naturally small seesaw neutrino mass with no new physics beyond the TeV scale*, Phys. Rev. Lett. **86**, 2502-2504 (2001), [arXiv:hep-ph/0011121](#); Q. H. Cao, E. Ma and G. Shaughnessy, *Dark Matter: The Leptonic Connection*, Phys. Lett. B **673** (2009) 152, [arXiv:0901.1334](#).
- [10] P. Ciafaloni, A. Urbano, *TeV scale Dark Matter and electroweak radiative corrections*, Phys. Rev. **D82** (2010) 043512, [arXiv:1001.3950](#).
- [11] T. Sjostrand, S. Mrenna, P. Z. Skands, *PYTHIA 6.4 Physics and Manual*, JHEP **0605**, 026 (2006), [arXiv:hep-ph/0603175](#); T. Sjostrand, S. Mrenna, P. Z. Skands, *A Brief Introduction to PYTHIA 8.1*, Comput. Phys. Commun. **178**, 852-867 (2008), [arXiv:0710.3820](#).
- [12] P. Salati, *Indirect and direct dark matter detection*, Proceedings of the 2007 Cargèse Summer School: Cosmology and Particle Physics Beyond the Standard Models, [PoS\(cargese\)009](#).
- [13] J. F. Navarro, C. S. Frenk and S. D. M. White, *The Structure of Cs Dark Matter Halos*, Astrophys. J. 462 (1996) 563, [arXiv:astro-ph/9508025](#).
- [14] A. W. Graham, D. Merritt, B. Moore, J. Diemand and B. Terzic, *Empirical models for Dark Matter Halos. I. Nonparametric Construction of Density Profiles and Comparison with Parametric Models*, Astron. J. 132 (2006) 2685, [arXiv:astro-ph/0509417](#); J. F. Navarro *et al.*, *The Diversity and Similarity of Cold Dark Matter Halos*, [arXiv:0810.1522](#).
- [15] A. Burkert, *The Structure of dark matter halos in dwarf galaxies*, IAU Symp. 171 (1996) 175 [Astrophys. J. 447 (1995) L25].
- See also: P. Salucci and A. Burkert, *Dark Matter Scaling Relations*, [arXiv:astro-ph/0004397](#). G. Gentile, P. Salucci, U. Klein, D. Vergani and P. Kalberla, *The cored distribution of dark matter in spiral galaxies*, Mon. Not. Roy. Astron. Soc. 351 (2004) 903, [arXiv:astro-ph/0403154](#); P. Salucci, A. Lapi, C. Tonini, G. Gentile, I. Yegorova and U. Klein, *The universal rotation curve of spiral galaxies. II: The dark matter distribution out to the virial radius*, Mon. Not. Roy. Astron. Soc. 378 (2007) 41, [arXiv:astro-ph/0703115](#).

- [16] M. Cirelli *et al.*, *PPPC 4 DM ID: A Poor Particle Physicist Cookbook for Dark Matter Indirect Detection*, [arXiv:1012.4515](https://arxiv.org/abs/1012.4515).